Structure-guided design of C3-branched swainsonine as potent and selective human Golgi α-mannosidase (GMII) inhibitor

Koemans, T.S.; Bennett, M.; Guimaraes Da Lomba Ferraz, M.J.; Armstrong, Z.W.B.; Artola Perez de Azanza, M.E.; Aerts, J.M.F.G.; ... ; Davies, G.J.

ChemComm

COMMUNICATION

View Article Online
View Journal | View Issue

Cite this: *Chem. Commun.*, 2024, **60**, 11734

Received 2nd September 2024,
Accepted 19th September 2024

DOI: 10.1039/d4cc04514a

rsc.li/chemcomm

Structure-guided design of C3-branched swainsonine as potent and selective human Golgi α-mannosidase (GMII) inhibitor†

Tony Koemans,‡[a] Megan Bennett,‡[b] Maria J. Ferraz,[a] Zachary Armstrong,[a] Marta Artola,[a] Johannes M. F. G. Aerts,[a] Jeroen D. C. Codée,[a] Herman S. Overkleeft*[a] and Gideon J. Davies*[b]

The human Golgi α-mannosidase, hGMII, removes two mannose residues from GlcNAc-Man$_5$GlcNAc$_2$ to produce GlcNAcMan$_3$GlcNAc$_2$, the precursor of all complex *N*-glycans including tumour-associated ones. The natural product GMII inhibitor, swainsonine, blocks processing of cancer-associated *N*-glycans, but also inhibits the four other human α-mannosidases, rendering it unsuitable for clinical use. Our previous structure-guided screening of iminosugar pyrrolidine and piperidine fragments identified two micromolar hGMII inhibitors occupying the enzyme active pockets in adjacent, partially overlapping sites. Here we demonstrate that fusing these fragments yields swainsonine-configured indolizidines featuring a C3-substituent that act as selective hGMII inhibitors. Our structure-guided GMII-selective inhibitor design complements a recent combinatorial approach that yielded similarly configured and substituted indolizidine GMII inhibitors, and holds promise for the potential future development of anti-cancer agents targeting Golgi *N*-glycan processing.

Swainsonine (**1**, Fig. 1) is a natural product indolizidine alkaloid and an inhibitor of the human Golgi α-mannosidase, hGMII (MAN2A1).[1,2] hGMII, a retaining glycoside hydrolase from the CAZyme family GH38, catalyzes the hydrolysis of both the terminal α-1,3-linked and α-1,6-linked mannoses from GlcNAcMan$_5$GlcNAc$_2$ *N*-glycans, which is essential for further processing towards complex *N*-glycoproteins. Alteration of *N*-glycan branching through GMII modulation impacts the metastatic potential of cancer cells, and for this reason swainsonine is an interesting starting point for the development of antitumor agents. Swainsonine has been subject to phase I and phase II clinical trials, but its nonselective inhibition of other human GH38 α-mannosidases (MAN2A2, MAN2B1, MAN2B2, MAN2C1) hampers its further development.[3] Specifically, inhibition of lysosomal α-mannosidase (MAN2B1) causes side-effects similar to the lysosomal storage disease, α-mannosidosis. Thus, swainsonine derivatives that selectively inhibit GMII without blocking the action of the other human mannosidases, and particularly that of the lysosomal mannosidase, MAN2B1, may succeed where swainsonine has failed in becoming effective, clinical anticancer agents.

hGMII, like the other human α-mannosidases, is a retaining exoglycosidase that cleaves substrate α-mannosides in a two-step, double displacement mechanism during which a transiently covalent enzyme–substrate adduct is formed. We recently developed a fluorescence polarization activity-based protein profiling (FP-ABPP) assay in which 358 glycomimetics were screened on their *Drosophila* GMII (dGMII) inhibitory potency.[4] This resulted in the discovery of several hits, including the micromolar inhibitors **2** and **3** (Fig. 1). These compounds capture different parts of swainsonine (**1**) with the swainsonine-configured

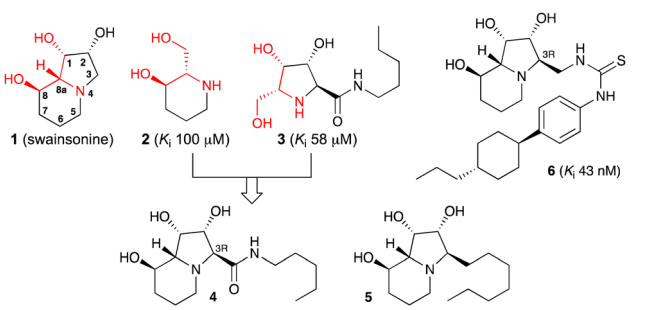

Fig. 1 Iminosugars subject to the here-presented studies: swainsonine (**1**), the piperidine (**2**) and pyrrolidine (**3**) fragments identified from our previous studies (K_i values for hGMII taken from the literature[4]) based on which we designed C3-branched, swainsonine-configured title compounds **4** and **5**. Similarly configured indolizidine **6** was recently[5] reported as a potent and selective competitive hGMII inhibitor in a natural product-driven combinatorial chemistry approach.

[a] *Leiden Institute of Chemistry, Leiden University, Einsteinweg 55, 2333 CC Leiden, The Netherlands. E-mail: h.s.overkleeft@lic.leidenuniv.nl*
[b] *Department of Chemistry, York Structural Biology Laboratory, The University of York, Heslington, York, YO10 5DD, UK. E-mail: gideon.davies@york.ac.uk*

† Electronic supplementary information (ESI) available. See DOI: https://doi.org/10.1039/d4cc04514a

‡ T. K. and M. B. contrinuted equally to this work.

2-amino-1,3-diol moiety (shown in red – the 1-8*a*-8 stretch) represented in both pyrrolidine and piperidine fragments. The remaining three carbons in piperidine **2** feature as C5–C6–C7 in swainsonine, and the remaining two pyrrolidine carbons in **3** as C2 (as secondary alcohol, with the same stereochemistry) and C3. In contrast to swainsonine, however, pyrrolidine **3** carries an exocyclic substituent at this C3 carbon. X-ray studies on dGMII (a close homologue of hGMII) complexed to either piperidine **2** or pyrrolidine **3** showed these fragments to occupy adjacent, partially overlapping positions within the enzyme active site. Moreover, the structure of dGMII complexed to **3** revealed the amide group of the appendage hydrogen bonded to the catalytic acid base residue. These data suggested that fusing the piperidine and pyrrolidine structural elements, while keeping the *trans*-configured (with respect to the 1,2-diol) C3 side chain functionality as in **3**, may lead to swainsonine analogues that inhibit GMII with improved selectivity. This idea was enforced by several studies[5–7] on C3-substituted swainsonine analogues, the most compelling of which is the recent report by Chen *et al.*[5] They identified in a natural product-inspired, computational chemistry guided combinatorial chemistry approach, a series of (3R)-substituted swainsonine derivatives including indolizidine **6** as a low nanomolar (K_i 0.043 μM) hGMII inhibitor with 106-fold selectivity over the other human α-mannosidases. With this reasoning in mind, we decided to 'grow' our pyrrolidine (**2**) and piperidine (**3**) fragments into full-fledged, C3-substituted swainsonines. This required an efficient route of synthesis, which we established for the preparation of compound **4** as depicted in Scheme 1.

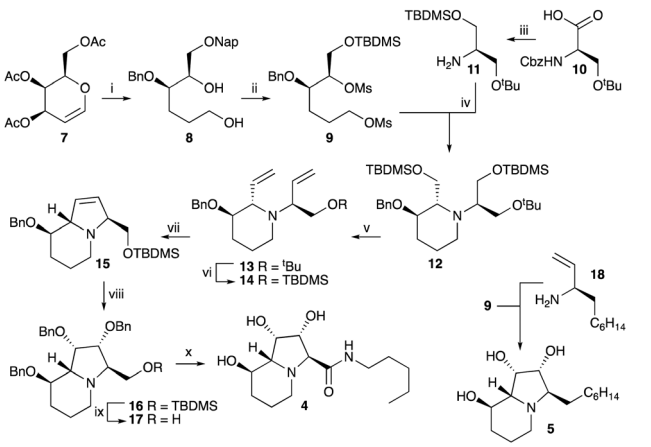

Scheme 1 *Reagents and conditions*: (i) 1. $SnCl_4$, iPrOH, DCM, r.t., 16 h, 62%; 2. H_2, Pd/C, EtOH, r.t., 3 h, 90%; 3. NaOMe, MeOH, r.t., 2 h, 99%; 4. NapBr, Taylor's catalyst, KI, K_2CO_3, MeCN, 65 °C, 3 h, 89%; 4. BnBr, NaH, TBAI, DMF, r.t., 16 h, 94%; 5. 4 : 1 AcOH/1 M HCl, 60 °C, 16 h, quant.; 6. $NaBH_4$, EtOH, r.t., 3 h, 98%; (ii) 1. MsCl, pyr, 0 °C, 2 h, quant.; 2. DDQ, 3 : 1 DCM/H_2O, r. t., 3 h, quant; 3. TBSCl, imidazole, DCM, 0 °C, 2 h, 96%; (iii) 1. Isobutyl chloroformate, *N*-methylmorpholine, $NaBH_4$, DCM, −15 °C, 2 h, quant; 2. TBSCl, imidazole, DCM, 0 °C to r.t., 2 h, 89%; 3. Pd/C, H_2, EtOH, r.t., 16 h, 98%; (iv) DIPEA, MeCN, 50 °C to 70 °C, 4 days, 77%; (v) 1. TBAF, THF, r.t., 16 h, 94%; 2. Oxalyl chloride, DMSO, Et_3N, DCM, −78 °C to 0 °C, 5 h; 3. $MeP(Ph)_3Br$, NaHMDS, THF, −78 °C to 0 °C, 16 h, 36% (over 2 steps); (vi) 1. TFA, H_2O, 0 °C to r.t., 2 h, 77%; 2. TBSCl, imidazole, DCM, 0 °C, 2 h, 94%; (vii) Schrock–Hoveyda catalyst, benzene, r.t., 16 h, 50%; (viii) 1. OsO_4, TMEDA, DCM, −78 °C, then ethylenediamine, r.t., 16 h, 48% (together with 16% stereoisomeric *cis*-diol); 2. BnBr, NaH, DMF, r.t., 4 h, 70%; (ix) TBAF, THF, r.t., 2 h, 82%; (x) 1. CrO_3, H_2SO_4, H_2O, acetone, 60 °C, 30 min, 42%; 2. Heptylamine, HATU, DIPEA, r.t., 16 h, 92%; 3. Pd/C, H_2, HCl, dioxane, r.t., 16 h, 89%.

The route of synthesis starts with a Ferrier rearrangement and subsequent protective- and functional group manipulations to transform tri-*O*-acetyl-D-galactal **7** into orthogonally protected 1,5-diol **8**. Bismesylation then gives intermediate **9**, which is susbsequently transformed, with inversion of stereochemistry at the secondary alcohol carbon, into piperidine **12** by double S_N2 displacement with secondary amine **11** (itself prepared in three steps from partially protected D-serine **10**). Removal of both silyl protective groups was followed by Swern oxidation of both primary alcohols, and then a double Wittig event to give diene **13**. At this stage and in the optimal route we swapped the *tert*-butyl ether for a TBDMS ether (**13** to **14**), for reasons explained further down. The subsequent ring-closing metathesis (RCM, **14** to **15**) proved far from trivial, and all Grubbs-type ruthenium catalysts we tried, also under conditions (addition of acid) that protects the catalyst from the free tertiary amine, proved abortive. Usage of Schrock's molybdenum catalyst fortunately proved productive, yielding indolizine intermediate **15** in decent (50%) and reproducible yield along with recovery of reusable starting material. The next key step – dihydroxylation – as well proved more eventful than anticipated. Here we found that the *tert*-butyl analogue of **15** (thus the RCM product of **13**, which can be obtained with equal efficiently), upon treatment with OsO_4 predominantly returns the epimeric (with respect to swainsonine) *cis*-diol. Treatment of **15** with OsO_4 and TMEDA followed by benzylation gave the desired protected *cis*-diol **16** as the major product, together with a significant portion of the epimeric one (3 : 1, 64% overall yield in this key step). Addition of ethylene diamine following the dihydroxylation step was required to break up the intermediate osmate ester, and for this reason stoichiometric OsO_4 was needed to achieve an effective dihydroxylation. Removal of the silyl protective group followed by Jones oxidation of the resultant primary alcohol **17**, condensation of the carboxylic acid with heptylamine and final global hydrogenolytic deprotection yielded target indolizidine **4**.

With the aim to demonstrate the generality of the route of synthesis, we prepared similarly configured indolizidine **5**, now by reacting bismesylate **9** with allylamine **18** with the alkyl sidechain already installed. The ensuing route of the thus obtained piperidine (see the ESI† for details) towards indolizidine **5** proceeded through the same general sequence of events (liberation of the diol, double Swern oxidation followed by double Wittig olefination, then RCM and then dihydroxylation) with comparable efficiency as described for **12**.

With branched swainsonines **4** and **5** in hand, we then determined their inhibition constants, together with that of swainsonine **1** as inhibitors of both hGMII and dGMII in a fluorogenic substrate assay with concentration-dependent inhibition of enzymatic 4-methylumbelliferyl-α-D-mannoside (4-MU-α-D-man) hydrolysis as the readout. Both enzymes are potently inhibited by swainsonine (K_i hGMII 40 nM, K_i dGMII 20 nM). As we reported previously,

piperidine **2** (K_i hGMII 100 μM, K_i dGMII 58 μM) and pyrrolidine **3** (K_i hGMII 41 μM, K_i dGMII 11 μM) are about three-fold weaker inhibitors for both enzymes. 3(*R*)-heptyl-swainsonine **5** (K_i hGMII 308 μM, K_i dGMII 167 μM) actually turns out to be a weaker inhibitor compared to the two fragments. Amide-modified swainsonine **4** in contrast (K_i hGMII 15 μM, K_i dGMII 6 μM) is somewhat (relative to pyrrolidine **3**) to considerably (relative to piperidine **2**) more potent as inhibitor of both dGMII and hGMII. Besides the presence of a C3 sidechain, also the nature of this pharmacophore is therefore of influence on inhibition potency. This is supported by the work of Chen *et al.*[5] who performed extensive optimization studies on this part of the scaffold, arriving at the nanomolar hGMII inhibitor **6** (Fig. 1).

The selectivity of compound **4**, being the most potent of the two branched swainsonine derivatives, was determined next in a fluorogenic substrate assay side by side with swainsonine **1**, piperidine **2** and pyrrolidine **3**. For this, extracts of cells in which either of the five human α-mannosidases (MAN2A1/hGMII, MAN2A2, MAN2B1, MAN2B2, MAN2C1) were brought to overexpression are first treated with these competitive inhibitors at varying concentrations, and subsequently with 4-methylumbelliferyl α-D-mannoside. Swainsonine **1** was revealed to be the most potent hGMII inhibitor also in these assays (Table 1B, values for MAN2A1), with the inhibitory potency of compounds **2–5** towards overexpressed hGMII more or less following the trent observed for recombinant dGMII. We note that comparing trents and absolute values observed from the two assays should be done with caution: the origin (species) of the enzymes is different. As well, the second assay makes use of samples in which one mannosidase is brought to over-expression but in which the other four are also present at endogenous expression levels. Yet these assays do allow interpretation of some trents to evaluate whether our branched swainsonine derivatives hold merit as GMII-selective inhibitors. Which we believe is the case, to some extent. Swainsonine **1** is, besides MAN2A1 (hGMII), also the most potent inhibitor of MAN2A2 and MAN2B1 of the series, and together with pyrrolidine **3**, also the most potent MAN2B2 inhibitor. Rather strikingly, compound **3** proved to be the most potent MAN2C1 inhibitor, outperforming swainsonine **1** in this regard, with the other compounds inactive up until 100 micromolar. The reported broad spectrum activity of swainsonine **1** is therefore also apparent from these studies. Piperidine **2** proved inactive for all five enzymes and this holds true as well for alkylindolizidine **5**. Pyrrolidine **3** gives a mixed picture, and is besides being a remarkable MAN2C1 inhibitor also as noted on par with swainsonine for MAN2B2. It is 10-fold less active for hGMII (MAN2A1) in this assay compared to indolizidine **4**. This latter compound turns out to be the second-most active hGMII inhibitor after swainsonine in this assay, which matches the result from the kinetics assay on dGMII. It is also rather selective, although MAN2B2 and especially MAN2B1 are inhibited rather potently as well.

Aiming to further investigate the mode of action of these inhibitors we soaked dGMII with **4** and **5** to produce three complexed crystal structures resolved to 2.14 Å and 2.47 Å resolution respectively. Both **4** and **5** were only partially modelled with electron density missing for part of, or all of (in the case of **5**) the alkyl chain (see also the ESI†). As dictated by the stereochemistry at C3 it is likely that these alkyl chains point towards the ''+1'' sugar binding pocket but due to the likely flexibility of these chains, and their inability to be resolved in the electron density, we cannot be completely certain. Unsurprisingly, the structure of these complexes resembled typical GH38 family type folds, with DALI servers[8] identifying high structural similarity to other GH38 enzymes such as bovine lysosomal α-mannosidase (PDB: 1O7D, 27% sequence identity, rmsd of 2.0 Å across 250 Cα residues[9]) and *Streptococcus pyogenes* α-mannosidase (PDB: 2WYH, 14% sequence identity, rmsd of 3.3 Å across 905 Cα residues).[10] Both dGMII and ligand contribute in coordinating the active site zinc,[4] and the octahedral zinc complex is formed by the 1- and 2-hydroxyls of the pyrrolidine ring together with His90, Asp92, Asp204 and His471 (Fig. S5, ESI†). The overall binding motif of **4** and **5** emulates that of swainsonine; coordinated by a series of hydrogen bonds in the active site (Fig. S6 (ESI†) and Fig. 2A). These hydroxyls on the pyrrolidine ring are also within hydrogen bonding distance of Asp92, Asp204 and Asp472. The hydroxyl attached to C1 of the piperidine fragment is hydrogen bonded to Asp472 and Tyr727. This hydrogen bonding network is also seen separately for each of the piperidine and pyrrolidine iminosugar fragments **2** and **3** (Fig. 2B and C).[4] The nitrogen of the ring in both **4** and **5** is coordinated by hydrogen bonds of approximately 2.7 Å and 3.2 Å respectively, from Asp204 (Fig. S6, ESI†). Compound **4** displays a K_i, towards both dGMII and hGMII >20-fold higher than that of compound **5**. The additional hydrogen bond between the amide of **4** and acid/base residue Asp341, which is absent for compound **5** (Fig. S6 (ESI†) and Fig. 2), may explain this difference in inhibitory potency. This

Table 1 (A) Inhibition constants (K_i values in μM) of swainsonine 1, piperidine 2, pyrrolidine 3 and branched indolizidines 4 and 5 as dGMII and hGMII inhibitors. (B) IC_{50} values for compounds **1–5** in lysates of human epithelial cells overexpressing MAN2A1/hGMII, MAN2A2, MAN2B1, MAN2B2 or MAN2C1

	A		B				
	dGMII	hGMII	MAN2A1	MAN2A2	MAN2B1	MAN2B2	MAN2C1
1	0.08 ± 0.008	0.04 ± 0.009	2.4 ± 0.2	30 ± 3.0	1.6 ± 0.06	15 ± 0.6	24 ± 0.5
2	58 ± 3	100 ± 7	>100	>100	>100	>100	>100
3	10.8 ± 0.8	41 ± 3	98 ± 16	>100	58 ± 2.6	13 ± 0.25	0.12 ± 0.007
4	5.6 ± 0.6	15 ± 5	9.1 ± 2.0	66 ± 11	24 ± 1.3	1.5 ± 0.05	>100
5	167 ± 13	308 ± 7	102 ± 12	>100	>100	>100	>100

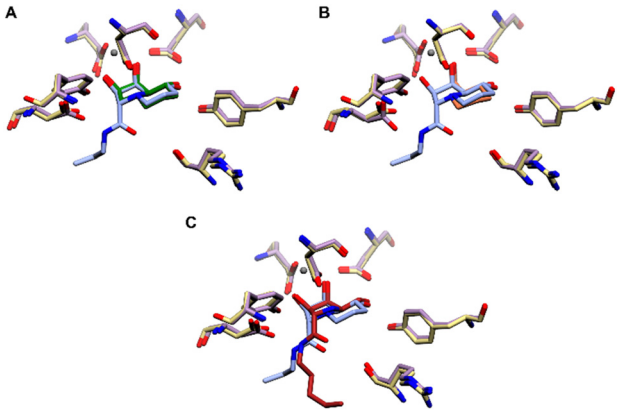

Fig. 2 Comparison of the binding pockets of dGMII in complex with inhibitors **1–4**. Images were created and visualised in CCP4mg (v. 2.10.11). The structure of **4** is displayed in blue cylinder form throughout. (A) Binding pocket of dGMII:**4** with active site residues (yellow) SSM superimposed with the binding pocket of dGMII (lilac residues) in complex with 1 (green) (PDB: 3BLB). (B) Binding pocket of dGMII:**4** with active site residues (yellow) SSM superimposed with the binding pocket of dGMII (lilac residues) in complex with inhibitor **2** (orange) (PDB: 6RRX). (C) Binding pocket of dGMII:**4** with active site residues (yellow) SSM superimposed with the binding pocket of dGMII (lilac residues) in complex with inhibitor **3** (red) (PDB: 6RRN).

interaction also appears in other lyxo-configured pyrrolidine inhibitors such as **3** and other previously reported low μM inhibitors (Fig. 2).[4] By molecular docking, Chen and coworkers uncovered a hydrogen bonding network to exist between Tyr354 and a thiourea substituent in one of their inhibitors.[5] We do not observe this hydrogen bonding in our inhibitors with the corresponding residue (Tyr269 from dGMII) being positioned >4 Å away from any possible coordinating partner such as the amide nitrogen in **4** or nitrogen in the bicyclic ring of both **4** and **5**. Additionally, Chen and colleagues noticed the occurrence of Sigma–π interactions and hydrophobic interactions between the 4-alkylcyclohexyl substituent in **6** with Tyr352/His358 and Gln150/Tyr316 in hGMII. They did not observe these interactions with hLM (MAN2B1), which may explain improved selectivity of this inhibitor for hGMII.

In conclusion, we here report a flexible and convergent strategy for the synthesis of C3-substituted swainsonines, which we demonstrate here in the synthesis of indolizidines **4** and **5**. Underscoring the literature report on the more elaborate indolizidine **6**,[5] compound **4** proves both more potent and more selective than the piperidine (**2**) and pyrrolidine (**3**) fragments as hGMII inhibitor. Structural studies corroborate the hypothesis behind our studies and indolizidine **4** occupies the partially overlapping sites where we previously[4] found compounds **2** and **3** to reside. The structural overlap with the swainsonine **1** bound structure is remarkable and additional interactions with the indolizidine **4** exocyclic amide bond with the enzyme active site likely contribute to the enhanced inhibitor potency (note that indolizidine **5** with a simple alkyl chain branch is less active). Chen and co-workers recently demonstrated that elaboration at this position yields nanomolar, selective hGMII inhibitors.[5] They arrived at the same 3(R)-substituted swainsonine scaffold following a strategy totally different from ours: combinatorial and natural product-inspired *versus* fragment based and structure-guided. Our approach supports the notion that hGMII, which has for several decades been regarded as a potential drug target, is druggable: compounds may be discovered that are selective for GMII over the four other human α-mannosidases.[11–13] Besides this, we feel our approach, selecting hits from our pyrrolidine/piperidine iminosugar library in an FP-ABPP assay, and then in a structure-guided fashion elaborate these hits to arrive at more potent and more selective inhibitors, should translate well to other disease-related glycosidases.

G. J. D. thanks the Royal Society for the Ken Murray Research Professorship. H. S. O thanks the Netherlands Organization for Scientific Research (NWO TOP grant 2018-714.018.002 to H. S. O.). We thank the European Research Council (ERC-2011-AdG-290836 "Chembiosphing" to H. S. O. and ERC-2020-SyG-951231 "Carbocentre" to G. J. D. and H. S. O.). We thank Diamond Light Source for beamtime (proposals mx932736-9 and mx32736-5), and the staff of beamline i03 for assistance with crystal testing and data collection. We thank Johan Turkenburg and Sam Hart for coordinating X-ray data collection.

Data availability

The data supporting this article have been included as part of the ESI.†

Conflicts of interest

There are no conflicts to declare.

References

1 S. M. Colegate, P. P. Dorling and C. R. Huxtable, *Aust. J. Chem.*, 1979, **32**, 2257–2264.
2 P. E. Goss, M. A. Baker, J. P. Carver and J. W. Dennis, *Clin. Cancer Res.*, 1995, **1**, 935–944.
3 P. E. Shaheen, W. Stadler, P. Elson, J. Knox, E. Winquist and R. M. Bukowski, *Invest. New Drugs*, 2005, **23**, 577–581.
4 Z. Armstrong, C.-L. Kuo, D. Lahav, B. Liu, R. Johnson, T. J. M. Beenakker, C. de Boer, C.-S. Wong, E. R. van Rijssel, M. F. Debets, B. I. Florea, C. Hissink, R. G. Boot, P. P. Geurink, H. Ovaa, M. van der Stelt, G. M. van der Marel, J. D. C. Codée, J. M. F. G. Aerts, L. Wu, H. S. Overkleeft and G. J. Davies, *J. Am. Chem. Soc.*, 2020, **142**, 13021–13029.
5 W. Chen, Y. Chen, C. Hsieh, P. Hung, C. Chen, C. Chen, J. Lin, T. Cheng, T. Hsu, Y. Wu, C. Shen and W. Cheng, *Chem. Sci.*, 2022, **13**, 6233–6243.
6 E. J. Hembre and W. H. Pearson, *Tetrahedron*, 1997, **53**, 11021–11032.
7 W. H. Pearson and L. Guo, *Tetrahedron Lett.*, 2001, **42**, 8267–8271.
8 L. Holm, A. Laiho, P. Törönen and M. Salgado, *Prot. Sci.*, 2023, **32**, e4519.
9 P. Heikinheimo, R. Helland, H. S. Leiros, I. Leiros, S. Karlsen, G. Evjen, R. Ravelli, G. Schoehn, R. Ruigrok, O. Tollersrud, S. McSweeny and E. Hough, *J. Mol. Biol.*, 2003, **327**, 631–644.
10 M. D. L. Suits, Y. Zhu, E. J. Taylor, J. Walton, D. L. Zechel, H. J. Gilbert and G. J. Davies, *PLoS One*, 2010, **5**, e9006.
11 See for recent related studies: J. Kóňa, S. Šesták, I. B. H. Wilson and M. Poláková, *Org. Biomol. Chem.*, 2022, **20**, 8932–8943.
12 M. Kalník, S. Šesták, J. Kóňa, M. Bella and M. Poláková, *Beilstein J. Org. Chem.*, 2023, **19**, 282–293.
13 M. Kalník, P. Gabko, J. Kóňa, S. Šesták, J. Moncol and M. Bella, *Bioorg. Chem.*, 2024, **150**, 107578.